Theoretical Penning electron-energy distributions for alkali-metal atoms: He(2 $^{1,3}S$) collisions with sodium and potassium

N. T. Padial, James S. Cohen, and Richard L. Martin
Theoretical Division, Los Alamos National Laboratory, Los Alamos, New Mexico 87545

Neal F. Lane
Department of Physics and Rice Quantum Institute, Rice University, Houston, Texas 77251
(Received 30 January 1989)

Penning electron-energy distributions are calculated for collisions of He(2 ^1S) and He(2 ^3S) with sodium and potassium atoms. The formulation is in terms of quantum-mechanical wave functions, which are determined using previously published complex potentials for the initial states and available experimental or presently calculated Hartree-Fock potential curves for the final state. Sensitivities to these potentials are tested. The mechanisms for the observed energy structure are analyzed, and the effects of experimental finite energy resolution and collisional velocity spread on the structure are shown.

I. INTRODUCTION

The collision of an excited atom A^* with a target atom B can result in the Penning ionization (PI) process,[1-3]

$$A^* + B \rightarrow A + B^+ + e^- , \quad (1)$$

if the excitation energy of A^* is greater than the ionization potential of B. The atom A is usually chosen as one of the long-lived metastable species, He(2 ^1S) or He(2 ^3S), whose excitation energies, 20.6 and 19.8 eV, respectively, exceed the first ionization energy of every neutral atom other than He and Ne. The related process of associative ionization results in the molecular ion AB^+.

Measurement and subsequent analysis of the Penning electron-energy distribution (PEED) give considerable information about the ionization collision dynamics as well as about the pertinent interaction potentials.[1-6] However, PEED spectra have rarely been calculated from *ab initio* potential curves and collision theory.[7,8] Nevertheless, calculation of the PEED presents an exacting additional test of the theory. The goal of the present study is to provide better understanding of the aspects of the collision dynamics that are most important in predicting the PEED, in particular for collisions of He* with alkali-metal atoms.

The optical model,[9] applied to the computation of either the total ionization cross sections or the PEED requires the initial-channel potential curve $V^*(R)$ and the transition rate $\Gamma(R)/\hbar$. Accurate calculations of $V^*(R)$ require large configuration-interaction (CI) electronic structure computations. Models and simplified *ab initio* prescriptions have been proposed that yield total PI cross sections in reasonable agreement with the experiments.[1,2] However, accurate *ab initio* calculations demand large basis sets including a large number of diffuse functions to represent the electronic continuum. Various L^2 approximations have been devised for calculating the widths $\Gamma(R)$.[10,11] The only supplemental information necessary for the PEED calculation is the final-state potential curve $V^+(R)$, which can be obtained through standard electronic structure techniques, e.g., Hartree-Fock or CI calculations.

Penning ionization of alkali-metal atoms by metastable He has received significant attention in recent years. Besides Penning-ionization electron spectroscopy,[6,12] other experimental methods used include the crossed-beam technique,[13,14] stationary-afterglow measurement,[15] and spin polarization of Penning electrons.[16] In addition, the experimental analysis of the energy spectra of electrons released from alkali-metal atoms incident on metal surfaces[17-19] is of current interest. The theoretical counterpart comprises a classical treatment[20] of the total ionization cross sections of Na for collisions with metastable He and the more elaborate calculations using *ab initio* optical potentials and widths for the ionization of sodium[21] and potassium[22] atoms.

In a recent paper,[23] we reported that the potential curves correlating with the lowest atomic autoionizing state and initial Penning state do not cross; therefore, inelastic transitions involving the atomic autoionizing states are expected to be unimportant. In the present work, we take into account the effect of finite resolution in the measurements of the electron energies as well as the effect of averaging over the distribution of the collision energies. For collisions of metastable He with the alkali-metal atoms, the final-state potential curves (e.g., for $HeNa^+$ and HeK^+) are shallow, and hence the associative ionization cross sections are expected to be very small, so we need not consider this process.

In Sec. II, we briefly describe the theoretical formulation and the approximations used. In Sec. III, we discuss the potential curves adopted in this paper. We present the results in Sec. IV and the conclusions in Sec. V.

II. THEORY

Hickman and Morgner[7] presented a comprehensive description of the theory of Penning ionization within the Born-Oppenheimer approximation as derived by several authors.[9,24] We shall use their working formula for the PEED (atomic units are used throughout, except when specifically indicated otherwise),

$$\frac{d\sigma(E,\varepsilon)}{d\varepsilon}=\frac{4\pi}{k^2}(2\mu)^2\left[\frac{1}{2\pi}\right]\sum_l(2l+1)e^{-2\,\mathrm{Im}\delta_l}\left|\int\xi_\varepsilon^l(R)\Gamma(R)^{1/2}\xi_d^l(R)dR\right|^2, \tag{2}$$

where ξ_d^l is the partial-wave solution to a single-channel Schrödinger equation with complex potential $V^*(R)-\frac{1}{2}i\Gamma(R)$, δ_l is the complex phase shift, ξ_ε^l is the partial-wave solution to a single-channel Schrödinger equation with potential $V^+(R)$, μ is the reduced mass of the system, $E=k^2/2\mu$ is the initial relative collision energy, and ε is the Penning electron energy. The nuclear rotation is included in the initial and final channels through a rotational centrifugal energy term $l(l+1)/2\mu R^2$.

The expression in Eq. (2) is quantum mechanical but still incorporates a few approximations. First, we assume that the initial and final partial-wave functions have the same l, i.e., the small amount of angular momentum carried away by the Penning electron is neglected. This approximation is necessary since the partial (l-dependent) widths have not been calculated. Because the sum in Eq. (2) includes a large number of partial waves (e.g., $l_{\max}\approx 200$ at thermal energies), this approximation is reasonable. Second, we assume that the electronic coupling of the initial state to the final state can be represented by a real R-dependent quantity $\Gamma(R)$, i.e., any R-dependent phase is neglected. To the best of our knowledge, this phase has never been calculated for any Penning ionization reaction, so it is difficult to say how much effect it might have. It is easiest to understand the possible effect of such a phase in terms of a stationary-phase argument. If there is more than one point of stationary phase associated with a given electron energy ε (often there are two), some error will be caused by this approximation to the extent that the phase varies. A third, related approximation, well justified by the stationary phase, entails the use in the calculation of $\Gamma(R)$ of a continuum state at exactly the energy $V^*(R)-V^+(R)$.

In the present treatment, both the initial- and final-state wave functions ξ_d^l and ξ_ε^l are obtained by solving the Schrödinger equation using the Numerov algorithm. Conservation of energy requires that

$$\frac{k_f^2}{2\mu}=\frac{k^2}{2\mu}+\varepsilon_0-\varepsilon\ , \tag{3}$$

where $k_f^2/2\mu$ is the asymptotic kinetic energy in the final state, and

$$\varepsilon_0=V^*(\infty)-V^+(\infty)\ . \tag{4}$$

As a test of our computer code, we repeated the calculations of Waibel *et al.*[8] on He^*+H. First, we calculated the associative ionization cross sections at the collisional energies of 0.01, 0.05, 0.08, 0.10, and 0.15 eV. The difference between our results and their results is less than 0.5% in every case except at 0.08 eV, where it is 1.0%. Waibel *et al.* separated the calculation of the Penning ionization into two parts: Penning and quasiassociative, in which the final quasi-bound-states are treated as bound states. We use the same process to calculate the electron-energy distribution in both regimes. To obtain

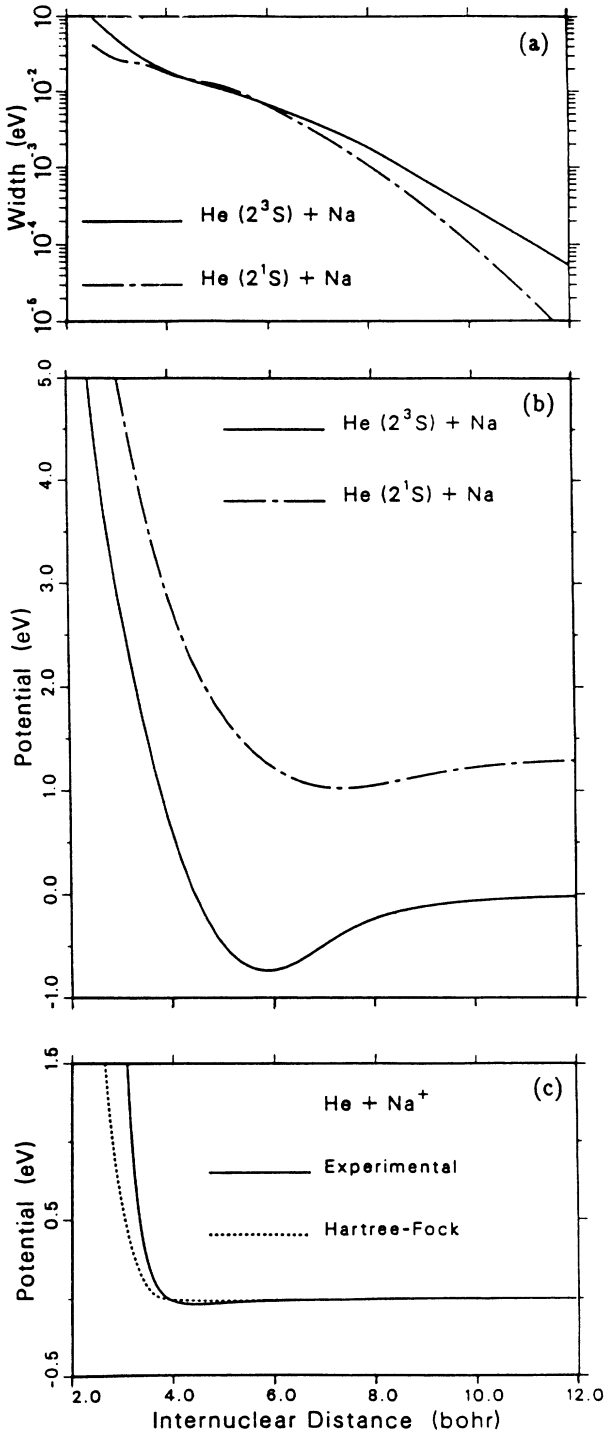

FIG. 1. (a) Stieltjes widths for $He(2\,^3S)+Na$ (solid) and for $He(2\,^1S)+Na$ (long and short dash); (b) potential curves for $He(2\,^3S)+Na$ (solid) and for $He(2\,^1S)+Na$ (long and short dash); (c) potential curve for $He+Na^+$—experimental results of Ref. 26 (solid) and the Hartree-Fock calculation (dash).

the total cross section, we integrated the electron-energy distribution. This integration requires a large number of Penning electron energies due to the resonances of the quasiassociative regime. In the position of each quasi-bound-state, we have very narrow resonances. We did the calculation at 0.5 eV for 2550 Penning electron energies. The value obtained integrating the electron-energy distribution was $98.10a_0^2$. This value compares well with the published value of $98.35a_0^2$ [$(91.20+7.15)a_0^2$)].

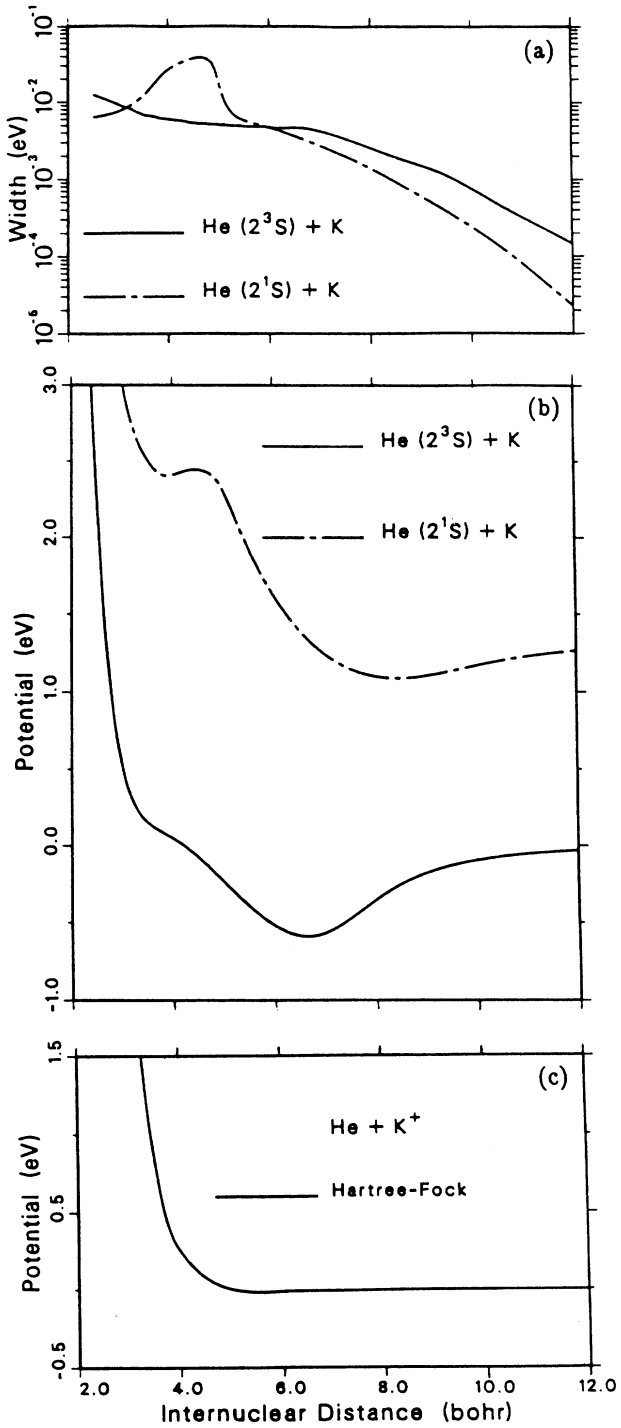

FIG. 2. Same as Fig. 1 but for He+K.

III. POTENTIAL

For $He^* + Na$ we adopt the $V^*(R)$ curves and widths of Cohen *et al.*[21] In that work, *ab initio* potential curves were first calculated using a moderate-sized CI calculation and then adjusted to yield the experimental well depth[12] and the correct asymptotic van der Waals form. The curves are shown in Fig. 1(b). The widths, which were obtained from a Stieltjes analysis[11,25] of a discrete representation of the $e^- + HeNa^+$ continuum, are shown in Fig. 1(a). Using the same basis as Cohen *et al.*,[21] we obtained the Hartree-Fock curve for $HeNa^+$ that is compared with the experimental results of Mason and Schamp[26] in Fig. 1(c). Since both atoms are closed shell in this case, the Hartree-Fock approximation is reasonably good.

For $He^* + K$, we used the adjusted CI potential curves and the widths of Scheibner *et al.*,[22] who took the same approach as Cohen *et al.*[21] Scheibner *et al.*[22] obtained a curve crossing between the Penning state $He(2\,^3S) + K(3p^6 4s)$ and the atomic autoionizing state $He(1s^2) + K(3p^5 4s^2)$ that had the effect of increasing the total ionization cross section slightly. However, we have reported[23] a more accurate calculation that shows that such a crossing is unlikely. We have also calculated a Hartree-Fock potential curve for HeK^+, using the same basis as Scheibner *et al.*[22] The initial-state interatomic potentials, the widths, and the final-state ionic potential are plotted in Fig. 2.

IV. RESULTS

A. $He^* + Na \rightarrow He + Na^+ + e^-$

We have calculated the PEED's for $He(2\,^1S, 2\,^3S) + Na$ at the average experimental collision energy of 0.071 eV, employing the potential curves and autoionization widths of Cohen *et al.*[21] and the experimental ion curve of Mason and Schamp[26] for $Na^+ + He$. The individual partial-wave terms in Eq. (2) exhibit rapid oscillations corresponding to the nodes in the initial- and final-state wave functions. Most of this structure is washed out in the sum over a larger number of partial waves, but that which remains is physically interesting and will be discussed in detail. The results of Eq. (2) are plotted in Figs. 3 and 4. We have also calculated the Hartree-Fock ion curve for the final state. The differences between the energy distributions obtained using the experimental and Hartree-Fock ion curves are too small to be observed in the graphs, being less than 1% in the singlet case. For the triplet case, the distribution is very slightly shifted to the left, i.e., to lower electron energies. In both cases, a more accurate calculation for the final state seems unnecessary. In fact, as a test of sensitivity, we used $V^+(R)=0$, and found that the distribution resulting from this extreme choice of ion curve looks very much like the other two, but is shifted to the left by about 0.03 eV. The reason for this insensitivity is that the classical turning

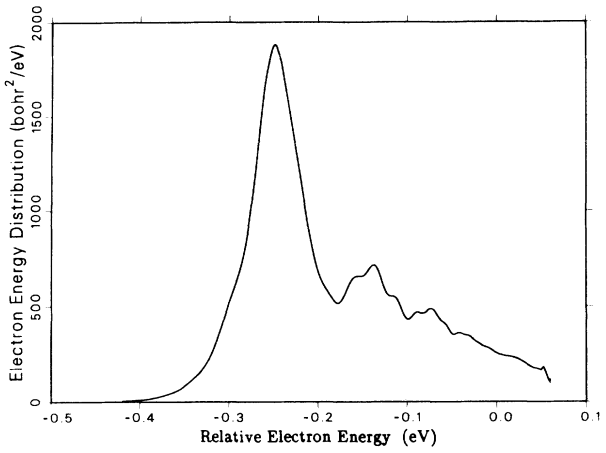

FIG. 3. Penning electron-energy distribution as a function of relative electron energy ($\varepsilon-\varepsilon_0$) using the theoretical V^* and the experimental V^+ for He($2\,^1S$)+Na.

point of the initial-channel (upper) potential curve lies to the right of the region in which the experimental and Hartree-Fock ion (lower) curves differ considerably. In addition, both curves are very close to zero outside this small internuclear separation region. The total ionization cross section depends strongly on the magnitude of the width function, but the electron-energy distribution is also very sensitive to the *shape* of the width function.

The theoretical PEED's exhibit rich structure that has not been observed in the experimental results,[6] presumably because the latter are smoothed by the finite energy resolution in the detection of the Penning electrons. Ruf *et al.*[6] estimated their effective resolution to be between 55 and 105 meV full width at half-maximum (FWHM). Using a Gaussian distribution with these respective values for the FWHM, centered at each point of our PEED, we obtain the results of Fig. 5. As we shall show for He*+K, the use of the average collision energy does not significantly modify the shape of the distributions.

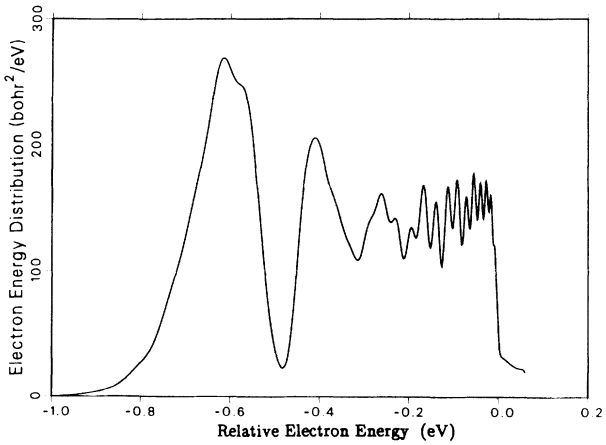

FIG. 4. Same as Fig. 3 but for He($2\,^3S$)+Na.

For the collision of the He($2\,^1S$) with Na, the resulting shape of the theoretical spectrum agrees well with the experiment. For the collision of He($2\,^3S$) with Na, the agreement is fair, but the structure appears to be rather more prominent in the theoretical curve.

To analyze the shape of the electron-energy distribution for He($2\,^3S$)+Na, we evaluated separately the contributions of different regions of internuclear separation R to the PEED. Specifically, we find the partial distribution obtained by calculating the integral of Eq. (2) with limits that correspond to different intervals: (i) [0,5]; (ii) [7, ∞]; (iii) both of the former intervals in the same calculation, i.e., *excluding* [5,7]; and (iv) [5,7]. In Fig. 6(a), we show the partial distributions for the cases (i), (ii), and (iii). In Fig. 6(b), we show the result of case (iv), and we also reproduce the total PEED of Fig. 4 in order to facili-

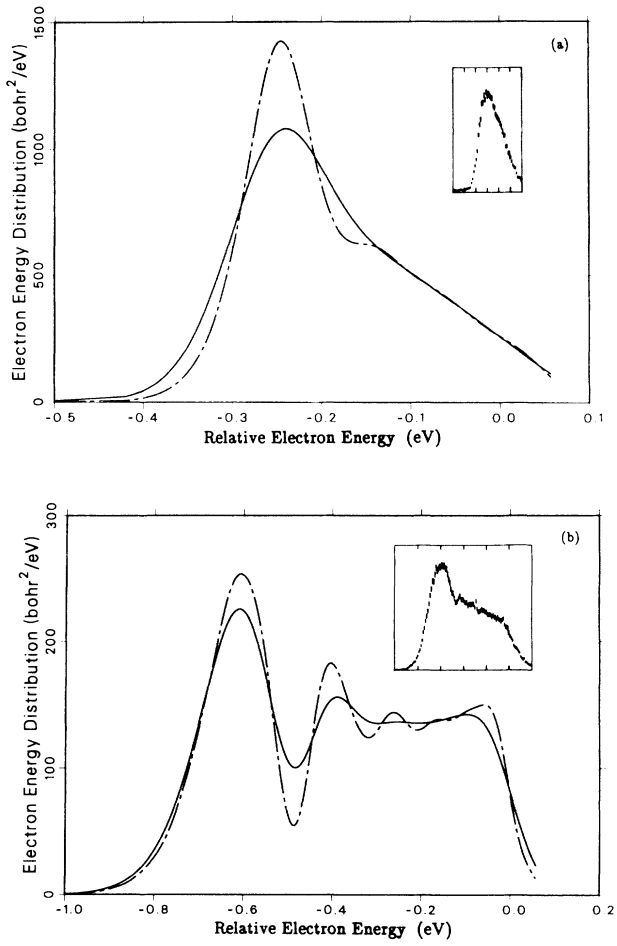

FIG. 5. Penning electron-energy distributions for (a) He($2\,^1S$)+Na and (b) He($2\,^3S$)+Na convoluted with the detector function. The energy resolutions are 105 meV (solid) and 55 meV (long and short dash). The insets show the experimental (Ref. 6) PEED's. The energy axes of the insets have the same values as the full frames at the corresponding tick marks, but the units of the experimental PEED's and aspect ratios are arbitrary.

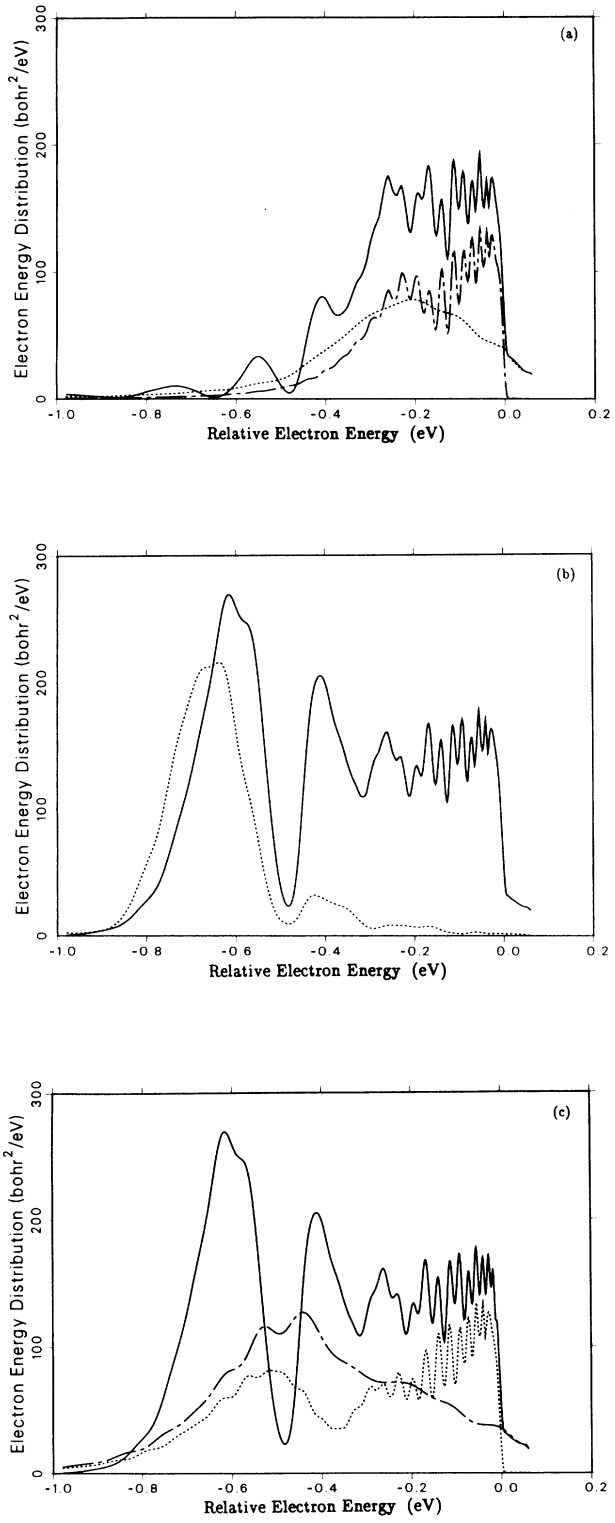

FIG. 6. Contribution of different parts of the potential to the electron-energy distribution for $He(2\,^3S)+Na$. The integral limits for Eq. (2) are in part (a) [0,5] (dash), $[7,\infty]$ (long and short dash), and both former intervals together (solid); in part (b) [5,7] (dash) and $[0,\infty]$ (solid); and in part (c) $[0,R_0]$ (long and short dash), $[R_0,\infty]$ (dash), and $[0,\infty]$ (solid), where R_0 is the minimum of the potential curve at 5.78.

tate the comparison. It is clear from Fig. 6(b) that the central part of the potential well is primarily responsible for the large intensity centered around $\varepsilon-\varepsilon_0=-0.6$ eV. The lateral parts of the potential contribute at the higher electron energies; since fewer partial waves are able to penetrate the short-range part of the potential, the contribution from the outer region is relatively more important, as is evident in fig. 6(a). The rapid oscillatory structure at high electron energies that is apparent in both the total PEED in Fig. 6(b) and the partial contribution from the interval $[R_2,\infty]$ in Fig. 6(a) is due to interference between the amplitudes for ionization at a particular value of R corresponding to incoming and outgoing trajectories.

Other aspects of the interference structure are demonstrated in Fig. 6(c), which shows the contribution from (i) $[0,R_0]$ and (ii) $[R_0,\infty]$, and (iii) the total distribution $[0,\infty]$, where $R_0=5.78$ is the minimum of the initial potential curve. Because the final potential curve is essentially flat in the relevant region, a given electron energy can occur only once in either of the branches (i) or (ii); hence it is clear that the structure in either of these two curves must arise from interference between the incoming and outgoing trajectories (semiclassically speaking) at the *same* R value. Indeed, the rapid oscillations evident in the $[R_0,\infty]$ contribution are the same as described above. On the other hand, in the total electron-energy distribution (iii), the pronounced maxima at ~-0.6 and ~-0.4 eV as well as the minimum at ~-0.5 eV must arise from interference between the amplitudes for ionization occurring at two *different* R values (two-point interference) since the structure is not already present in (i) or (ii). At the first maximum this interference is completely constructive, whereas at the first minimum it is completely destructive. The position of the deep minimum is insensitive to the collision energy. At the high electron energies, interference between the two waves at the *same* R value (single-point interference) is most important. The high electron energies come primarily from ionization at large R where the derivative of the potential curve is small and hence larger ΔR (and consequently larger phase accumulations) are required for a given $\Delta\varepsilon$; hence the energy period of the oscillations decreases as ε increases. At intermediate energies, both types of interference are important and the superposition displays irregular structure. Even though a large number of partial waves are required to converge the cross sections, the interference structure does not wash out. Semiclassical calculations carried out to examine this interference effect exhibit the same qualitative behavior.

In order to glean a further qualitative understanding of the complex form of the electron-energy distribution, we can consider the form of the integral in Eq. (2), which involves the product of the initial- and final-state heavy-particle wave functions and the square root of the width. For a given calculation of the PEED, we fix the initial energy of the collision, He^*+Na, at $k^2/2\mu$ and sweep through a range of electron energies ε by varying the energy of the final nuclear state $k_f^2/2\mu$ [see Eq. (3)]. Therefore, in evaluating the integral for a particular partial wave l, the quantity $\xi_d^l(R)\Gamma(R)$ remains fixed while $\xi_\varepsilon^l(R)$

varies with changes in the final-state energy. Since the ion potential-energy curve is quite flat, we can, for present purposes, take it to be zero, i.e., $V^+(R)=0$. In this case, the final-state wave function has the particularly simple form $\xi_\varepsilon^l(R)\approx k_f R j_l(k_f R)$, where j_l is a spherical Bessel function of order l. *Just for purposes of illustrating the nature of the problem,* we take $l=0$ and the width as a constant and further assume that the upper curve is also a constant, so the wave functions are simply $\xi_d^0(R)\approx\sin(kR)$ and $\xi_\varepsilon^0(R)\approx\sin(k_f R)$. As k_f approaches k, the fixed wave number for the initial state, the two functions begin to constructively interfere, and the integral in Eq. (2) grows in magnitude. The maximum in this integral is reached when the two energies are equal. Therefore, as a function of the final wave number k_f, we would observe a peak in the electron distribution at $k_f=k$. In this trivial case, the peak in the PEED would occur at $\varepsilon=\varepsilon_0$.

Of course, the initial-state potential curve is actually far from constant. We may crudely view it as having only two distinct regions: (i) a deep attractive component of limited range, say $[R_1,R_2]$, and (ii) a broader, shallow region $[R_2,\infty]$. (We ignore the region $[0,R_1]$ for this discussion.) We may consider the particle to have an effective radial kinetic energy and corresponding momentum characteristic of each of these two regions. In the first region, the effective energy will be of the form $k_1^2\approx k^2+2\mu|V^*|$. However, because the initial energy is much smaller than the depth of the potential, the effective energy is determined mainly from the interaction potential, i.e., $k_1^2\approx 2\mu|V^*|\gg k^2$. Away from the well, where V^* is small, particularly in the region $[R_2,\infty]$, the effective kinetic energy and momentum depend more sensitively on the asymptotic energy, i.e., $k_2^2\approx k^2$. The phase matching between the final-state wave function, which is basically a pure sine wave for $l=0$, and these two identifiable segments $[R_1,R_2]$ and $[R_2,\infty]$ of the fixed initial-state function leads to two distinct peaks in the electron distribution, corresponding respectively to the sharp peak in Fig. 6(b) arising from the region [5,7] and the broad peak in Fig. 6(a) arising from the region $[7,\infty]$. The high-electron-energy peak corresponds to the low-energy (i.e., low k_2) final heavy-particle states, while the low-electron-energy peak corresponds to the high-energy heavy-particle states. Since many partial waves are involved and since this dichotomy in the contributing regions of the potential is not really sharp, the actual distribution has a more complicated form. However, the basic two-peak structure is still readily discernible. An interesting confirmation of this simple explanation comes from the partial-wave analysis. At larger l, the heavy particles are excluded from the inner region of V^*, including, at sufficiently high l, the region around the well. In this case, we observe that the peak associated with k_1 eventually disappears.

We have carried out calculations that demonstrate that agreement between the theoretical and experimental results in Fig. 5(b) for He($2\,^3S$) can be improved either by modifying the potential *or* the width so as to minimize the importance of large R and thereby make the second peak relatively less important. This can be accomplished by either reducing the width at large values of R or by making the potential more attractive outside its minimum to reduce the time spent in this region, but the present calculations are not able to decide between these two alternatives.

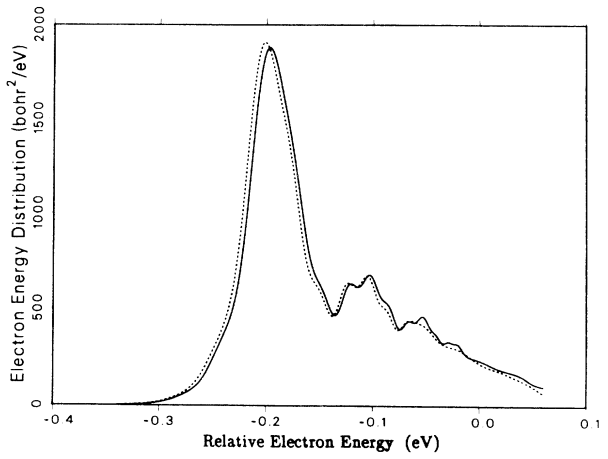

FIG. 7. Penning electron-energy distributions for He($2\,^1S$)+K using the Hartree-Fock V^+ (solid) and $V^+=0$ (dash).

The lack of prominent structure in the theoretical He($2\,^1S$) PEED is due in part to its larger van der Waals coefficient (3660 a.u. as opposed to 2220 a.u. for the triplet). Consequently higher partial waves are able to penetrate the region just outside the potential minimum and result in electrons that tend to fill the large hole that persists in the He($2\,^3S$) PEED at about -0.5 eV. The remaining structure is not resolved by the assumed spectrometer.

B. $He^*+K\rightarrow He+K^++e^-$

For the He^*+K reaction, we adopted the theoretical

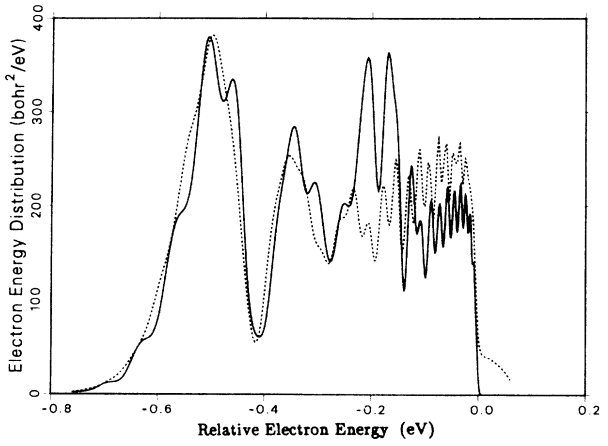

FIG. 8. Same as Fig. 7 but for He($2\,^3S$)+K.

potential curves and the widths calculated by Scheibner *et al.*[22] for the upper electronic state and the Hartree-Fock curve for the ion. As before, we focus on the average collision energy of the most recent experimental data,[6] which is 0.067 eV. The results are plotted in Figs. 7 and 8.

We also took into account the finite experimental electron-energy resolution as we did before. The results are illustrated in Fig. 9. Finally, we investigated the effects of averaging over the collision-energy distribution. We assumed a Maxwellian distribution for the K beam with the experimental temperature of 750 K, and a Gaussian distribution for the metastable He beam corresponding to an experimental average velocity of 1757 m/s and an experimental velocity width[6] $\Delta v/\bar{v}_{\mathrm{He}}$ (FWHM) of 31%. With these two distributions, we determined the effective distribution

$$D(v)=\int D_g(\mathbf{v}_{\mathrm{He}})D_M(\mathbf{v}_{\mathrm{K}})d\mathbf{v}_{\mathrm{He}} , \tag{5}$$

where D_g is the Gaussian distribution, D_M is the Maxwellian distribution, and $\mathbf{v}_{\mathrm{K}}=\mathbf{v}+\mathbf{v}_{\mathrm{He}}$.

With the distribution normalized to that $\int D(E)dE=1$, where E is the collision energy, the velocity-averaged PEED is given by

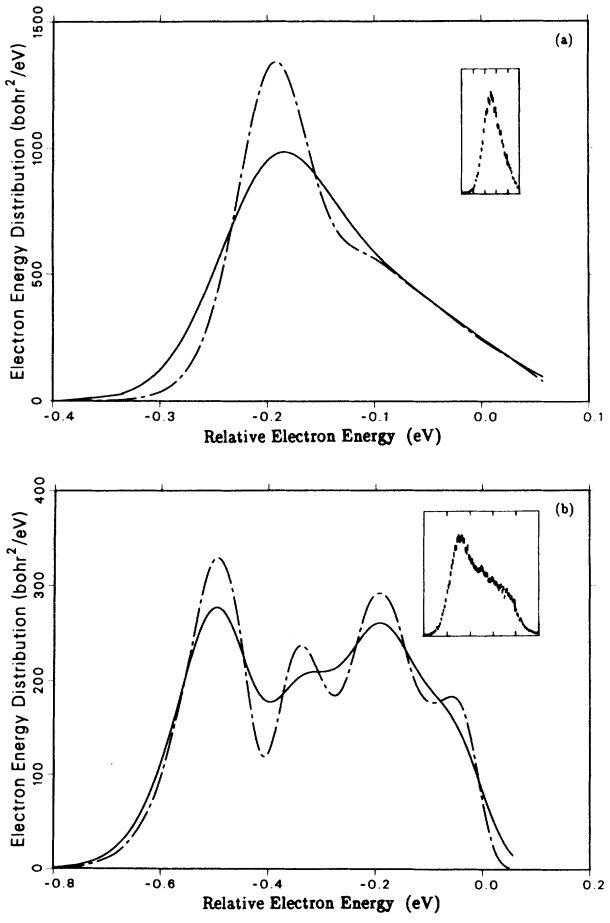

FIG. 9. Same as Fig. 5 but for He^*+K.

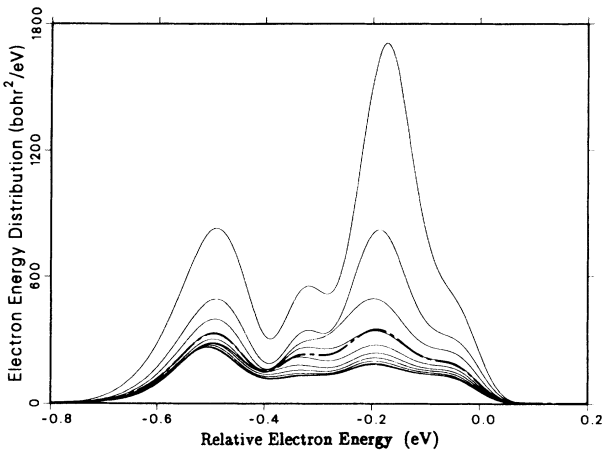

FIG. 10. Penning electron-energy distributions for $He(2\,^3S)+K$ with a detector energy resolution of 80 meV. The light curves show the cross sections for the several energies (0.002 54, 0.010 62, 0.025 24, 0.044 60, 0.067 00, 0.090 44, 0.112 84, 0.132 20, 0.146 81, and 0.155 38 eV) used to calculate the average (the heavy long and short dashed curve).

$$\frac{d\bar{\sigma}(\varepsilon)}{d\varepsilon}=\int \frac{d\sigma(E,\varepsilon)}{d\varepsilon}D(E)dE . \tag{6}$$

We calculated $d\sigma(E,\varepsilon)/d\varepsilon$ for the triplet He metastable collision at the relative energies necessary for a ten-point Gaussian quadrature of Eq. (6). Since the raw distributions have such a rapidly varying structure, we used in the final integral the distribution convoluted with the electron-energy resolution function. In Fig. 10, we show the average PEED as a heavy dashed curve superimposed on the individual cross sections used in the calculation.

For $He(2\,^1S)+K$, the agreement of the calculated PEED with the experimental shape[6] is good, as in the case of Na, but for $He(2\,^3S)+K$ the theoretical curve shows considerably more intensity at the higher electron energies (especially $\varepsilon-\varepsilon_0\approx-0.2$ eV) than does the experimental curve. As for $He(2\,^3S)+Na$, the agreement between the theoretical and experimental results could be improved by modifying *either* the potential or the width, so we do not present such an empirical adjustment.

V. CONCLUSIONS

Penning electron-energy distribution (PEED) calculations provide an exacting test of the potential-energy and autoionizing-width curves used to theoretically describe the Penning-ionization collision process. However, it is still not generally possible to infer uniquely these curves from the experimental data, even though the situation is simplified for metastable helium collisions with alkali-metal atoms by the flatness of the final-state potential curve. The present calculation of the PEED is completely quantum mechanical, and the results are expected to be almost as good as the curves used. The convolution of the theoretical spectrum with the experimental resolution function has been found to be essential for understanding the observed shape, but the averaging over collision-

energy distribution has little qualitative effect.

The experimental PEED's for singlet metastable helium exhibit no structure for any of the alkali-metal atoms; on the other hand, the PEED's for triplet metastable helium show some structure for every alkali-metal atom, including a shoulder on the high-energy side of the spectra.[6] The experimental energy measurement is not sufficient to resolve most of the calculated structure. Our calculated PEED shapes for collisions of He($2\,^1S$) with sodium and potassium atoms are in agreement with the experimental shapes. However, the calculated shapes for He($2\,^3S$) with potassium, and to a lesser extent sodium, contain more high-electron-energy intensity and display more structure than the experimental distributions, even after the smoothing corresponding to the stated experimental conditions. It is interesting to note that such pronounced structure is present in the experimental PEED for He($2\,^3S$) with lithium.[6]

On the experimental side, higher-resolution Penning electron spectra would certainly be useful, since the present resolution washes out most of the calculated structure. On the theoretical side, further progress depends on the more accurate calculation of the energies and widths of the Penning resonance states.

ACKNOWLEDGMENTS

This work was performed under the auspices of the U.S. Department of Energy. One of us (N.F.L.) was supported in part by the U.S. Office of Basic Energy Sciences, Division of Chemical Sciences and by the Robert A. Welch Foundation. We thank Paul Clark for carrying out related semiclassical calculations and Lee Collins for helpful discussions.

[1]A. Niehaus, Adv. Chem. Phys. **45**, 399 (1981), and references therein.

[2]B. M. Smirnov, Usp. Fiz. Nauk **133**, 569 (1981) [Sov. Phys.—Usp. **24**, 251 (1981)].

[3]A. Niehaus, in *Physics of Electronic and Atomic Collisions,* edited by S. Datz (North-Holland, Amsterdam, 1982), p. 237.

[4]A. J. Yencha, in *Electron Spectroscopy: Theory Techniques and Application,* edited by C. R. Brundle and A. D. Baker (Academic, New York, 1984), Vol. 5, p. 197.

[5]J. Lorenzen, H. Hotop, and M.-W. Ruf, Z. Phys. D **1**, 261 (1986).

[6]M. -W. Ruf, A. J. Yencha, and H. Hotop, Z. Phys. D **5**, 9 (1987).

[7]A. P. Hickman and H. Morgner, J. Phys. B **9**, 1765 (1976).

[8]H. Waibel, M. -W. Ruf, and H. Hotop, Z. Phys. D **9**, 191 (1988).

[9]W. H. Miller, J. Chem. Phys. **52**, 3563 (1970).

[10]A. P. Hickman, A. D. Isaacson, and W. H. Miller, J. Chem. Phys. **66**, 1483 (1979).

[11]A. U. Hazi, J. Phys. B. **11**, L259 (1978).

[12]H. Hotop and A. Niehaus, Z. Phys. **238**, 452 (1970).

[13]H. Haberland and W. Weber, J. Phys. B **13**, 4147 (1980).

[14]Y. A. Tolmachev and D. Fogel, Opt. Spektrosk. **48**, 818 (1980) [Opt. Spectrosc. (USSR) **48**, 451 (1980)].

[15]C. E. Johnson, C. A. Tipton, and H. G. Robinson, J. Phys. B **11**, 927 (1978).

[16]L. G. Gray, R. S. Keiffer, J. M. Ratliff, F. B. Dunning, and G. K. Walters, Phys. Rev. A **32**, 1348 (1985).

[17]J. Lee, C. Hanrahan, J. Arias, F. Bozso, R. M. Martin, and H. Metiu, Phys. Rev. Lett. **54**, 1440 (1985).

[18]B. Woratschek, W. Sesselmann, J. Juppers, and G. Ertl, Phys. Rev. Lett. **55**, 611 (1985).

[19]B. Woratschek, W. Sesselmann, J. Kuppers, and G. Ertl, Phys. Rev. Lett. **55**, 1231 (1985).

[20]V. P. Zhadanov and M. I. Chibisov, Opt. Spektrosk. **41**, 521 (1976) [Opt. Spectrosc, (USSR) **41**, 307 (1976)].

[21]J. S. Cohen, R. L. Martin, and N. F. Lane, Phys. Rev. A **31**, 152 (1985).

[22]K. F. Scheibner, J. S. Cohen, R. L. Martin, and N. F. Lane, Phys. Rev. A **36**, 2633 (1987).

[23]N. T. Padial, R. L. Martin, J. S. Cohen, and N. F. Lane, Phys. Rev. A **39**, 2715 (1989).

[24]H. Nakamura, J. Phys. Soc. Jpn. **26**, 1473 (1970); **31**, 574 (1971).

[25]P. W. Langhoff, Chem, Phys. Lett. **22**, 60 (1973); and in *Electron and Photon Molecule Collisions,* edited by T. Rescigno, V. McKoy, and B. I. Schneider (Plenum, New York, 1979), p. 183.

[26]E. A. Mason and H. S. Schamp, Jr., Ann. Phys. (N.Y.) **4**, 233 (1958).